IEEE Access
Multidisciplinary : Rapid Review : Open Access Journal

Received May 4, 2018, accepted May 30, 2018, date of publication June 8, 2018, date of current version July 6, 2018.

Digital Object Identifier 10.1109/ACCESS.2018.2845366

Numerical Improvement for the Mechanical Performance of Bikes Based on an Intelligent PSO-ABC Algorithm and WSN Technology

ZIDONG HAN[1], YUFENG LI[2], AND JUNYU LIANG[2]
[1]Department of Electrical and Electronic Engineering, Southern University of Science and Technology, Shenzhen 518055, China
[2]Shenzhen Hopnetworks Ltd., Shenzhen 518055, China

Corresponding author: Zidong Han (hanzd@sustc.edu.cn)

ABSTRACT This paper proposed a novel hybrid optimization algorithm, particle swarm optimization-artificial bee colony (PSO-ABC), based on the PSO and ABC algorithms. The ABC algorithm can offset defects in the PSO algorithm that easily fall into a local optimization; combining the algorithms can improve the optimization ability of the PSO algorithm to a certain extent. Therefore, this paper applied the PSO-ABC hybrid algorithm and the finite-element method to systematically optimize the mechanical performance of the disc rotor of a bike and verified the numerical computation model via the wireless sensor network technology. The experimental test was completed with wireless sensor network technologies. To verify the optimized effects of the proposed PSO-ABC hybrid algorithm after parameter selection, the algorithm was compared with the traditional PSO and ABC models. The PSO, ABC, and PSO-ABC models adopted the same population to conduct a multi-objective optimization for vibration accelerations of the disc rotor. Comparing the results from these models proved that the proposed PSO-ABC method is superior for the optimization of vibration characteristics of the disc rotors.

INDEX TERMS PSO algorithm, ABC algorithm, PSO-ABC hybrid algorithm, WSN technology, multi-objective optimization.

I. INTRODUCTION

In recent years, with increasing severity to problems such as traffic jams, energy shortages and environmental pollution, as well as the population's increasing desire for recreation and entertainment, bikes have gained more attention for development because of their small footprint, high flexibility and convenience, low cost, economic efficiency and durability, and ease of repair [1]–[5]. Bikes belong to a product category with very high requirements for dynamic performance and comfort. Vibration can cause physiological effects for a rider, which can then affect riding safety and bike operability and can reduce the service life of bike parts. Therefore, it is necessary to research and control vibration characteristics during bike riding to improve comfort and to increase the service life of bike parts.

Recently, research on the vibrations and dynamics of bikes has obtained significant achievements. Liu *et al.* [6] applied the finite element method to damaged mountain bikes and found that the stress concentration positions of a frame were consistent with the damage; the study further proposed three improvement proposals and compared the improvement results. Xiang *et al.* [7] adopted an experimental method to compare vibration characteristics of mountain bikes whose rear suspension was equipped with different types of dampers under different frequencies of harmonic excitation; the study found that a spring damper had good damping effects within a certain frequency scope. Nakae *et al.* [8] examined squeal and chatter phenomena generated experimentally in mountain bike disc brakes and found that there are two kinds of frictional self-excited vibrations in bike disc brakes: squeal (with frequency of 1000 Hz) and chatter (with frequency of 500 Hz). Covill *et al.* [9] outlined an FE model using beam elements to represent a standard road bicycle frame. The model simulates two standard loading conditions to understand the vertical compliance and the lateral stiffness characteristics of 82 bicycle frames from the bicycle geometry project to compare these characteristics with an optimized solution for these conditions. Based on the analysis of the dynamics of bikes, He *et al.* [10] proposed two weak-coupling dynamical sub-models, namely, a stability model

2169-3536 © 2018 IEEE. Translations and content mining are permitted for academic research only.
Personal use is also permitted, but republication/redistribution requires IEEE permission.
See http://www.ieee.org/publications_standards/publications/rights/index.html for more information.

and a vibration model, to describe bike motion under complicated road conditions. In combination with problems encountered in bikes use, such as structure, dynamics and vibration, Huang *et al.* [11] integrated ISIGHT with multidisciplinary optimization and selected a Nonlinear Programming by Quadratic Lagrangian (NLPQL) method for gradient optimization; the optimization results showed that the total mass of a bike frame should be decreased by 8.31% based on constraint condition satisfaction to achieve benefits from a lightweight frame. To discuss the dynamic performance of a bike main frame, Du *et al.* [12] applied ANSYS to analyze its elastic modal characteristics; the results showed that the finite element computation results were consistent with the experimental testing results. Combined with the vibration characteristics of the frame, modal sensitivity analysis technologies were applied to research the effects of bike frame wall thickness on the first-order modal frequency of bikes. Improving comfort in road bicycle design is a paramount concern for cyclists, who are affected by the vibrations caused by contact with the road surface. Therefore, Lépine *et al.* [13] presented two different laboratory techniques for studying road bike vibration. Caya *et al.* [14] investigated the influence of the dynamic behavior of a brake hood force transducer on measurement accuracy. However, most published references failed to conduct systematic research on and optimize the vibration of bike parts, and the results of numerical simulations were not experimentally verified. With regards to a few references that researched the optimization of bike vibration characteristics, the applied optimization algorithms were fairly traditional and could easily result in local extreme values, meaning the obtained results were not optimal.

With the function optimization of low-dimensional space, PSO is a quick solution that produces high-quality results. Nevertheless, once the dimensions of the function increase, PSO's optimization performance decreases sharply and could result in local extreme values, leading to a decrease in convergence accuracy and difficulty converging to a globally optimal solution; however, because of advantages such as few control parameters, easy achievement and concise computation, the method has been widely applied. ABC has outstanding capacity with balanced exploration and exploitation; however, due to the impact of evolution methods and selection strategies, the algorithm could easily result in local optima in rapid convergence. To overcome the defects of PSO and ABC (that each algorithm could easily result in local optimization when used separately), this paper proposed a novel hybrid optimization algorithm, PSO-ABC, based on PSO and ABC. The ABC algorithm can offset the defects of the PSO algorithm, which easily results in local optima. Combining the two could improve the optimization ability of the PSO algorithm to some extent. Therefore, this paper applied the PSO-ABC hybrid algorithm to systematically optimize bike vibration characteristics and to verify the accuracy of the numerical computation models generated via experimentation. The detailed contents in this paper are as listed: the second section introduced the finite element model of the bike, the third section has verified the numerical model using the wireless sensor network, and the other sections introduced the optimization process for the bike.

II. ESTABLISHMENT AND MODAL COMPUTATION OF THE FINITE ELEMENT MODEL

Bikes have complicated structures composed of many parts, most of which are revolving or thin-wall parts. Therefore, shell elements could be used to establish a finite element model. Fig. 1 shows a simplified geometric model of an actual bike. The model neglects some details. For example, some parts in the handle have been neglected, and the seat cover has been also neglected; thus, the modeling time could be reduced, and convergence failure could be avoided in numerical computations.

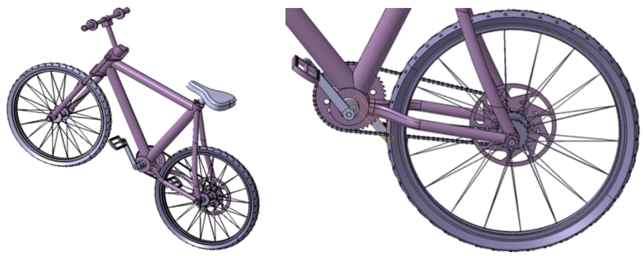

FIGURE 1. Simplified geometric model of a bike.

While developing a finite element model of a bike, the quantity of model elements has an obvious effect on the computational results and computational scale. In general, a higher number of elements leads to higher computation accuracy and an increase in the computational scale [15]–[20]. Therefore, impacts of the computational results and computational scale should be considered comprehensively to determine element quantity. ANSYS software can conduct rational mesh division of a complicated model, can find mistakes in mesh division, can control the size of local elements and can refine the mesh in key analysis areas. Through multiple division experiments, the mesh shape and size could be determined. To reduce computational complexity, the model should be simplified. It is necessary to ensure that basic attributes of the model, such as mass and rotation inertia, do not vary obviously before and after the simplification. Thus, structural simplification can be controlled within an allowable error scope.

The imbedded Mesh-Tool in ANSYS was used to assign element types, material attributes and element thicknesses for each bike part. To divide meshes rationally and effectively, the mesh size was set to the basic size (20 mm), according to an actual model. LESIZE was used to control some key lines. Mapped and Sweep were the first choice for mesh division manners. For a complicated model, Boolean calculations, such as "divide," could be used to divide the original model into regular shapes. Connections between each element assembly part play a crucial role in load transfer and degrees of freedom; thus, the mesh density is slightly higher in some parts compared to others. After mesh division of each module, it is necessary to couple and constrain their degrees of freedom through equivalent replacement according to the connections of the actual structure. Different shell elements were simulated by node coupling. Shell elements and solid elements were simulated by MPC. The imbedded contact pair tool in ANSYS, Contact Manager, was applied. Regarding the node-face contact pairs, the default target element was TARGET170, and the default contact element was CONTA175. Regarding the face-face contact pairs, the default target element was TARGET170, and the default contact element was CONTA174. Finally, the finite element model of the bike was obtained, as shown in Fig. 2. The model contained 56902 elements and 69026 nodes. In the finite element model, the density of the stainless-steel material was 7900 kg/m^3, its elasticity modulus was 210 GPa, and its Poisson's ratio was 0.3; the density of the rubber material was 1.5 kg/m^3, its elasticity modulus was 7.8 GPa, and its Poisson's ratio was 0.47.

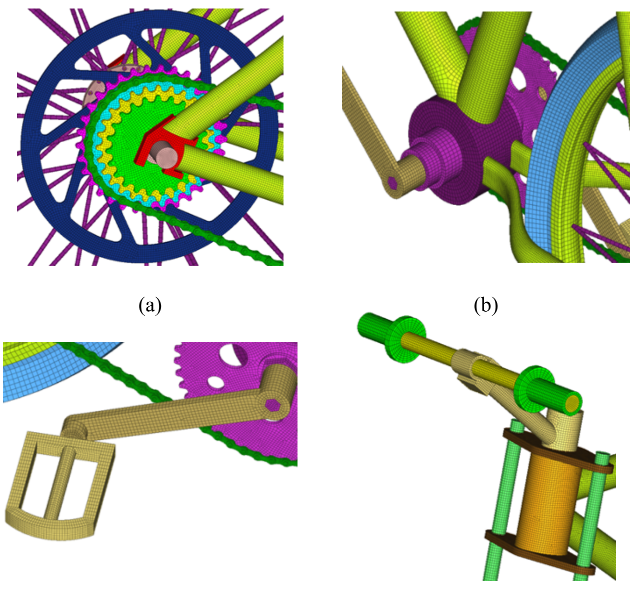
(a) (b) (c) (d)

FIGURE 2. Zoomed mesh drawings of an area of the bike. (a) Rear gears and disc rotor. (b) Crank. (c) Pedal. (d) Handlebars.

Structural modal analysis is the foundation of other dynamical analyses [21]–[23] and is a linear analysis. In the ANSYS software, it is used to determine natural frequency and vibrational modes of a structure. To solve for the natural characteristics of the bike, the modal parameters were obtained through modal analysis based on modal theories. In modal computation, vibration shapes of the bike could be obtained with a gradual approach at first. The Lance partition method is a modal extraction method with many functions, but it is most commonly used and applicable to general situations. In addition, other methods have unique advantages. For example, the downsizing method would have higher computation efficiency than other methods after defining the main degree of freedom of the bike (although the selection of the main degree of freedom requires careful consideration). Different methods are based on different algorithms. The Lance partition method is based on the Lance algorithm, whose calculation involves vector recursion and whose accuracy and computational efficiency could satisfy actual engineering requirements. Regarding large and symmetric models, the addition of a sparse equation could simplify the computational process. Because bikes are large and have similar front and rear structures, this paper selected this method for computation. Fig. 3 shows the top 9 orders of the natural vibration shapes of the bike obtained based on the Lance algorithm. The bike had many parts; therefore, most modal shapes were reflected in different partial structures of the bike. In addition, we can find that a series of bike vibrations appeared mainly at the front and rear wheels, and the disc rotor structure of rear wheel had obvious vibration.

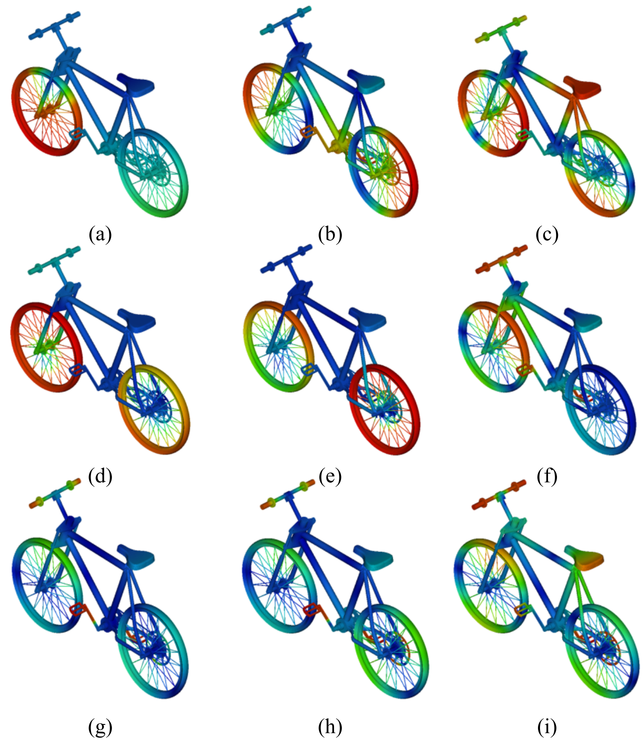
(a) (b) (c) (d) (e) (f) (g) (h) (i)

FIGURE 3. Natural vibration shapes of the top 9 orders of a bike. (a) First order. (b) Second order. (c) Third order. (d) Fourth order. (e) Fifth order. (f) Sixth order. (g) Seventh order. (h) Eighth order. (i) Ninth order.

III. EXPERIMENTAL VERIFICATION OF VIBRATION CHARACTERISTICS OF A BIKE USING WSN TECHNOLOGY

Some published papers concerning bike excitation loads obtained the excitation loads at the bike saddle. The excitation load was applied to the center of the saddle of the bike finite element model so that vibration acceleration responses of the bike could be computed. However, the computation model of bike vibrational responses is very complicated. Without experimental verification, the reliability of computational results may not be guaranteed. In addition, to increase the accuracy of the computational model, vibrational responses of multiple points on the bike should be verified. If a bike keeps running, a traditional wired sensor can be used to measure vibrational responses at multiple points on the bike, resulting in data lines that will be too long. Data lines between different sensors may be interweaved, thus influencing experimental testing and results. With rapid development and gradual maturity of communication technology, embedded computation technology and sensor technology, people have developed various microsensors with perception, computation capacity and communication capacity. A wireless sensor network (WSN) consisting of many microsensors has gained many attention [24]–[26]. Hence, multi-point vibrational responses of bikes can be tested with WSN technology. WSN integrates sensor technology, embedded computation technology, distributed information processing technology and communication technology [27]–[30]. It can assist in real-time monitoring, sensing and collection of information in various environments, monitor objects in a network distribution area and process the information. In this way, detailed and accurate information can be obtained and sent to users who need it. At present, WSN technology has been successfully applied to environmental monitoring, medical care, intelligent building and intelligent traffic, etc., as shown in Fig. 4.

FIGURE 4. The application of the wireless sensor network technologies.

The WSN system architecture used in this paper is shown in Fig. 5. This system is comprised of distributed wireless sensor node groups, sink nodes, a base station, transmission media and a network user side. The nodes are manually arranged on the bike. The sensor node network is taken as the core. In the sensing area, sensor nodes constitute the network; sensed information is sent to sink nodes. With the sink link, data in the entire area can be transmitted to the network user side for processing. During the experiment, the bike kept running. To verify the accuracy of the FE model, 10 sensor nodes were arranged in total. 5 sensor nodes were connected to 1 sink node; hence, 2 sink nodes were needed. These 2 sink nodes were connected to 1 base station. The base station transmitted the received data to the server and sed the Internet for subsequent data storage and analysis.

Computed and experimental RMS values at 10 monitoring points were extracted for comparison, as shown in Table 1. It is shown in the table that point 9 had the maximum

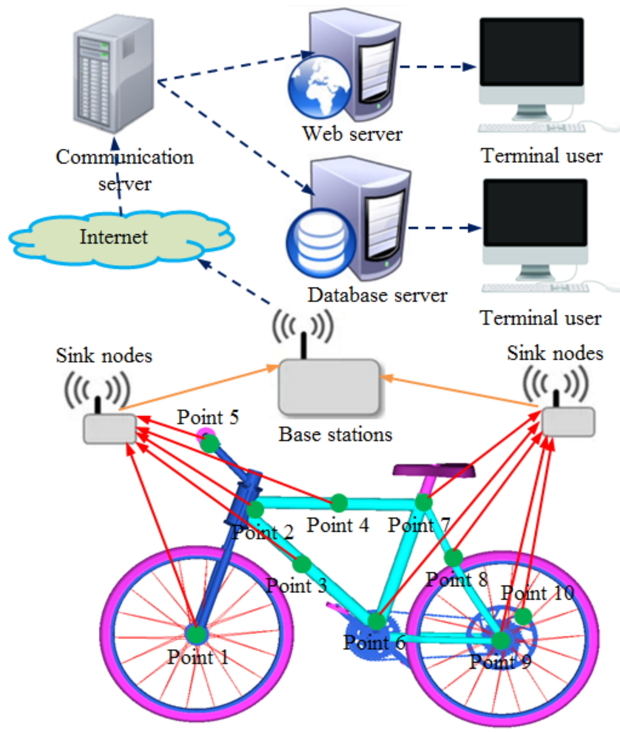

FIGURE 5. Experimental test of vibration accelerations of a bike using WSN technologies.

TABLE 1. Comparison of experimental results and numerical simulation of vibration accelerations.

Positions	Experimental test (m/s^2)	Numerical simulation (m/s^2)	Relative errors
Point 1	20.8	19.7	-5.23%
Point 2	16.5	17.1	3.64%
Point 3	17.9	18.7	4.47%
Point 4	17.2	17.8	3.49%
Point 5	8.3	7.9	-4.82%
Point 6	21.6	20.6	-4.63%
Point 7	19.1	19.9	4.19%
Point 8	23.2	22.1	-4.74%
Point 9	27.3	28.8	5.49%
Point 10	26.1	25.5	-2.30%

vibration acceleration response, while that of the rear wheel disk ranked second. The disk does not have the maximum vibrational response, but the disk is connected to the bike gear, so running safety and comfort of the bike will be influenced greatly, which can reduce the bike's service life. Hence, the vibrational response RMS value at this point was taken as the optimization objective. In addition, through extraction of the vibrational response curve of the disk, it was found that the difference between the maximum and minimum values of the vibration acceleration was quite large. Hence, riding comfort would be seriously affected and service life would be reduced. Hence, in this paper, with the exception of the vibrational response RMS value of the point taken as the optimization objective, the maximum difference in vibrational responses was taken as another optimization objective and the research became a multi-objective optimization issue.

IV. NUMERICAL OPTIMIZATION OF VIBRATION CHARACTERISTICS OF THE DISC ROTOR

The design variable of this paper is the thickness of all the parts connected to disc rotor. In this way, the structure does not need to be redesigned—only the thickness needs to be changed during the processing of the optimized part. The disc rotor has very large vibration accelerations, wherein the difference between the maximum and minimum vibration accelerations was very large. Therefore, the root-mean-square value and the maximum difference of the vibration accelerations are taken as optimization objectives and set as min(f). The following mathematic model was set:

$$\begin{cases} \min(f_1) = f(x_1, x_2, x_3, x_4) \\ \min(f_2) = f(x_1, x_2, x_3, x_4) \\ x_i^{(l)} \leq x_i \leq x_i^{(u)} \qquad\qquad i = 1, 2, 3, 4 \end{cases} \tag{1}$$

where f_1 is the root-mean-square value of vibration accelerations of the disc rotor, f_2 is the maximum difference of vibration accelerations of the disc rotor, x_i is a design variable, $x_i^{(l)}$ is the lower limit of the design variable and $x_i^{(u)}$ is the upper limit of the design variable.

Particle Swarm Optimization (PSO) is a random evolution algorithm based on swarm intelligence. This algorithm was proposed based on social behavior rules of bird, fish and human groups. The algorithm has drawn extensive attention within academia in recent years because of its quick convergence, fewer set parameters and simple implementation. PSO has been widely applied in function optimization, neural network training, mode classification, fuzzy system control and other engineering fields [31]–[36]. Traditional PSO achieves quick solutions and high-quality function optimization in low-dimensional space. However, once dimensions of the function increase, its optimization performance decreases sharply and it could easily result in local extreme values. As a result, convergence accuracy decreases and convergence to global optima would be difficult. The Artificial Bee Colony (ABC) algorithm is a random optimization algorithm based on swarm intelligence. The algorithm simulates honey collection behaviors of bee swarms. Bees conduct different activities according to labor division. Bee swarm information is shared and exchanged so that optimal solutions of problems could be found. At present, research and applications of ABC remains in the initial stage; however, it has drawn attention of scholars because of its advantages, such as few control parameters, easy implementation and concise computation. ABC has been successfully applied to problems in engineering fields, such as numerical optimization of functions and artificial neural network training [37]–[44]. The ABC effectively balances the abilities of exploration and exploitation; however, due to the effects of evolution modes and selection strategies, the algorithm could easily result in local optima during rapid convergence. To overcome the defect that PSO and ABC algorithms could easily result in local optima when separately applied to global optimization problems, this paper proposes a novel hybrid optimization algorithm based on PSO and ABC. The ABC algorithm could offset the issue of the PSO algorithm easily resulting in local optima. Through combination of these two algorithms, the optimization ability of the PSO algorithm could be enhanced to some extent. Therefore, PSO and ABC are mixed in parallel. A population is divided into 2 sub-populations. For each iteration, the ABC algorithm is applied to one sub-population to find the optimal solution and the PSO algorithm is applied to the other to find its optimal solution. The optimal solutions obtained for the two methods are compared and the global optimal solution is selected; the optimal solution is the global optimal solution in the iteration. The hybrid algorithm adopts the local and global search abilities of the ABC algorithm. Through continuous comparison, selection and abandoning of solutions, the search scope is reduced and the defect of the PSO algorithm (that it can result in local optima) can be overcame.

The optimal model is solved by the PSO-ABC hybrid algorithm. Specific processes are shown in Fig. 6.

With continuous maturing of commercial software, effective transmission parameter interfaces are set between different software. The commercial software could be integrated into ISIGHT software in a seamless manner and parameters could be analyzed in ISIGHT. Through modification of design parameters, a product model could be modified. With such automatic manner, complicated and repeated tasks in traditional design, such as continuous modification and checking, could be reduced and some tedious and complicated computations could be avoided. The method integrates the design processes to form a uniform frame and automatically operates simulation software and modifies parameter data. Based on the working principle, ISIGHT achieves full-course digitalization and automation of optimal design. During optimization with the ISIGHT optimization software, the PSO-ABC optimization algorithm proposed in this paper is implanted via ISIGHT secondary development. The ISIGHT software would modify all the integrated input parameters of the software, call solution software to solve them, read response results and judge if the response results are optimal. If the optimal solution is achieved, the optimization program will stop and the optimization will end. Otherwise, the parameters will be modified and responses will be solved and read again. Such a process is repeated and cycled continuously until an ideal target function value is obtained.

To further verify the validity of the PSO-ABC algorithm after parameter selection, the algorithm was compared with traditional PSO and ABC models. PSO, ABC and PSO-ABC models adopted the same population to conduct a multi-objective optimization for vibration accelerations of the disc rotor. The iteration processes of the three optimization algorithms are shown in Fig. 7. The ending condition of the iterations of the three algorithms was the reaching of a set proceeding generation. As shown in Fig. 7 that, the error convergence values were 0.145, 0.215 and 0.085, respectively, when iterations of PSO, ABC and PSO-ABC were conducted

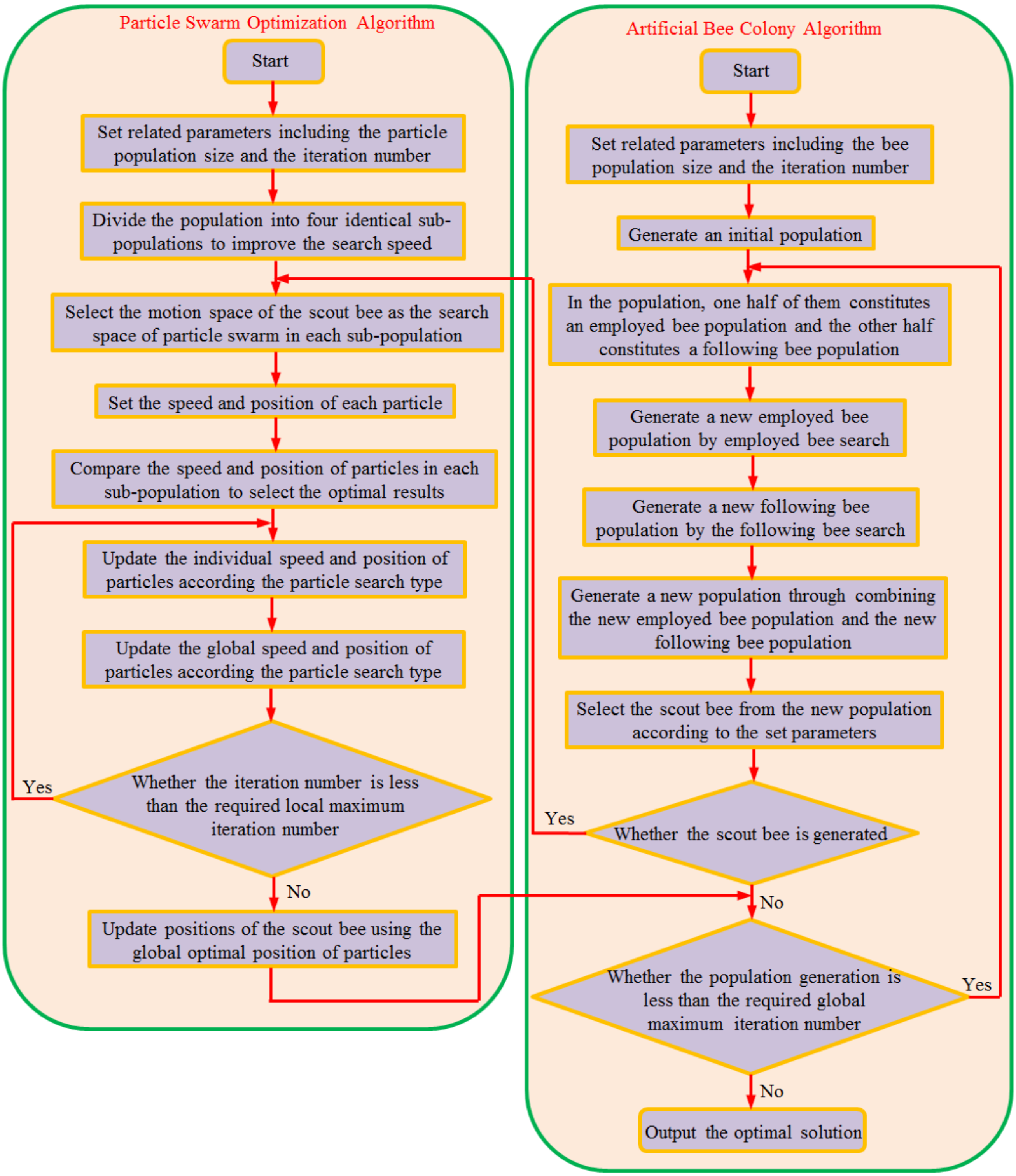

FIGURE 6. Specific processes of the PSO-ABC hybrid algorithm.

to the 70th generation, wherein all the values were not smaller than the set error critical value (0.01). When iterations were conducted to the 198th generation, the error of the PSO-ABC model was 0.009, which was smaller than the set critical error value (0.01). At this generation, errors of the PSO and ABC models were 0.135 and 0.095, respectively—far exceeding the critical error. When the iterations were conducted to 70th-360th generations, the PSO model resulted in local extreme

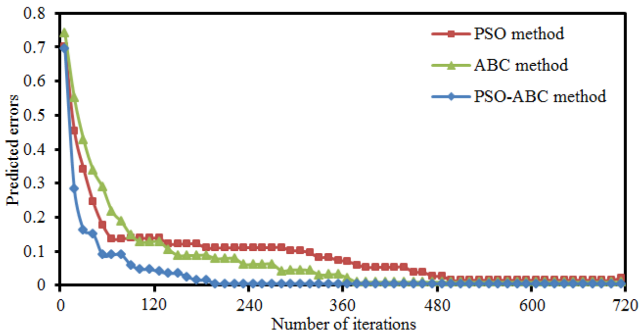

FIGURE 7. The iteration results of the three algorithms.

values and jumped from the local extreme values after long-term iterations. When the iterations were conducted to the 500^{th} generation, the PSO model converged and the error was 0.12, which still exceeded the set critical error. When the iterations were conducted to the 370^{th} generation, the ABC model converged and the error was 0.025, which exceeded the critical error. When iterations of the PSO-ABC model were conducted to the 198^{th} generation, the predicted error was smaller than the set critical error, the optimization accuracy improved and the time was reduced. To present optimal iterations of the three algorithms more visually, the root-mean-square value and the maximum difference of vibration accelerations were taken as horizontal and longitudinal coordinates respectively and a population figure of the disc rotor was obtained. The results are shown in Fig. 8. It is shown in Fig. 8 that performance of most individuals was better than performance of the original individuals during optimization. The maximum difference of original vibration accelerations was 68 m/s^2 and its root-mean-square value of vibration accelerations was 25.5 m/s^2. During optimization using the traditional PSO method, the maximum difference of vibration accelerations was 59 m/s^2 and the root-mean-square value of vibration accelerations was 22.5 m/s^2; the maximum difference of vibration accelerations decreased by 13.2% and the root-mean-square value of vibration accelerations decreased by 11.7%. During optimization using the ABC method, the maximum difference of vibration accelerations was 59.5 m/s^2 and the root-mean-square value of vibration accelerations was 22.3 m/s^2; the maximum difference of vibration accelerations decreased by 12.5% and the root-mean-square value of vibration accelerations decreased by 12.5%. During optimization using the PSO-ABC method, the maximum difference of vibration accelerations was 50.5 m/s^2 and the root-mean-square of vibration accelerations was 19.3 m/s^2; the maximum difference of vibration accelerations decreased by 25.7% and the root-mean-square of vibration accelerations decreased by 24.3%. Therefore, the PSO-ABC method is superior to the other two algorithms for the optimization of vibration characteristics of disc rotors.

A geometric model was re-established according to optimization parameters of the disc rotor, and the corresponding vibration acceleration computation model was obtained.

TABLE 2. Key iteration points of three kinds of optimization models.

Three kinds of optimization models	Number of iterations	Errors	Number of iterations	Errors
PSO model	70	0.145	720	0.120
ABC model	70	0.215	720	0.025
PSO-ABC model	70	0.085	198	0.009

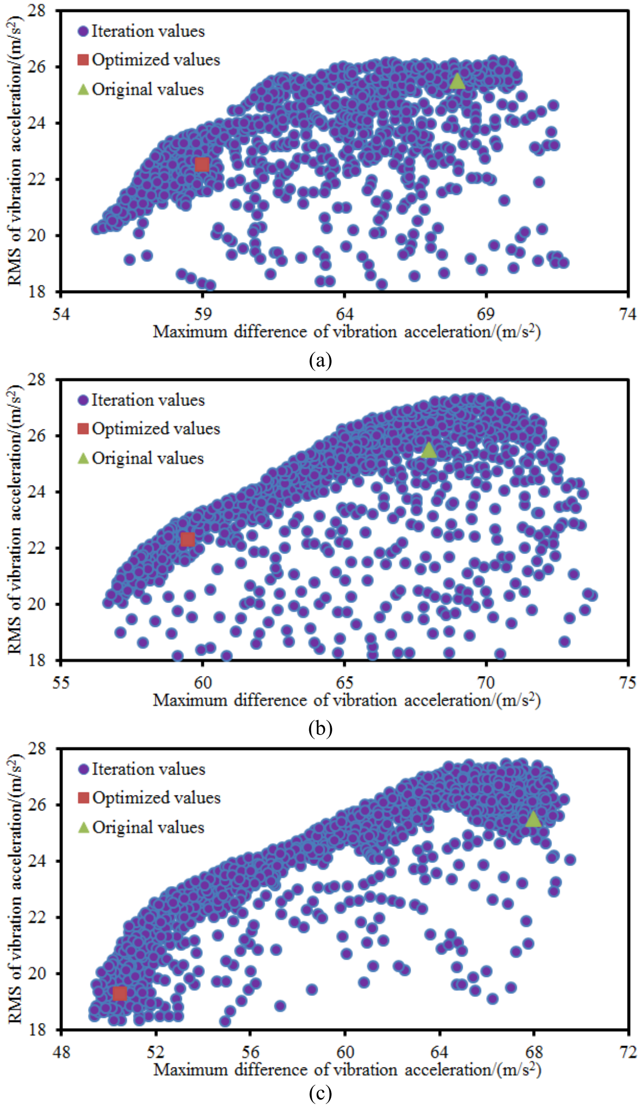

FIGURE 8. Bee swarm mutation processes of the three algorithms. (a) PSO method. (b) ABC method. (c) PSO-ABC method.

After computational optimization, the results of the disc rotor were compared with the original results, as shown in Table 3. It is shown in the table that the RMS value of the optimized disk vibrational responses was 19.5, which decreased by 23.5% from the original value; therefore, the optimization effect was significant. During optimization, vibrational response RMS values of some points increased, especially Point 5; however, the increase in amplitude was not very large. Vibrational responses of most points were improved. In addition, the maximum difference of optimized disk

TABLE 3. Comparison of original results and optimized results of vibration accelerations.

Positions	Original values (m/s^2)	Optimized values (m/s^2)	Optimized effects
Point 1	19.7	20.2	2.54%
Point 2	17.1	16.7	-2.34%
Point 3	18.7	17.9	-4.28%
Point 4	17.8	18.2	2.25%
Point 5	7.9	8.3	5.06%
Point 6	20.6	19.8	-3.88%
Point 7	19.9	19.1	-4.02%
Point 8	22.1	22.6	2.26%
Point 9	28.8	28.2	-2.08%
Point 10	25.5	19.5	-23.50%

vibrational responses was 50.5. The original value was 68. The relative decrease in amplitude was 25.74%. Therefore, the PSO-ABC multi-objective optimization algorithm proposed in this paper is superior to the traditional algorithms at improving bike vibration characteristics.

V. CONCLUSIONS

The bike had many parts; therefore, most modal shapes were reflected in different partial structures of the bike. In addition, found that a series of bike vibrations mainly appeared at the front and rear wheels, whereas the disc rotor structure of the rear wheel had obvious vibration. Vibration accelerations had consistently changing trends in the experimental test and the numerical simulation, whereas the accelerations did not differ substantially. Therefore, the numerical computation model established in the paper is feasible. Based on the verified model, the vibration characteristics of bikes were optimized by the proposed PSO-ABC algorithm. To further verify the validity of the PSO-ABC algorithm after parameter selection, the algorithm was compared with traditional PSO and ABC models. The PSO, ABC and PSO-ABC models adopted the same population to conduct a multi-objective optimization for vibration accelerations of the disc rotor. When iterations of the PSO-ABC model were conducted in the 132nd generation, the predicted error (0.001) was smaller than the set critical error, whereas the optimization accuracy was improved, and the time was reduced compared to the other two algorithms. Vibration accelerations of the optimized disc rotor were improved obviously. The maximum absolute value of vibration accelerations was 49.1 m/s^2, and the maximum absolute value of the vibration accelerations of the original structures was 59.0 m/s^2. Therefore, the PSO-ABC method was superior for the optimization of vibration characteristics of the disc rotor. In the future, we will try to compare this study with those more advanced algorithms to optimize the vibration performance of the bike further.

REFERENCES

[1] T. Raviv, M. Tzur, and I. A. Forma, "Static repositioning in a bike-sharing system: Models and solution approaches," *EURO J. Transp. Logistics*, vol. 2, no. 3, pp. 187–229, Aug. 2013.

[2] J. C. García-Palomares, J. Gutiérrez, and M. Latorre, "Optimizing the location of stations in bike-sharing programs: A GIS approach," *Appl. Geogr.*, vol. 35, nos. 1–2, pp. 235–246, 2012.

[3] H. R. Sayarshad, S. Tavassoli, and F. Zhao, "A multi-periodic optimization formulation for bike planning and bike utilization," *Appl. Math. Model.*, vol. 36, no. 10, pp. 4944–4951, Oct. 2012.

[4] L. Caggiani and M. Ottomanelli, "A modular soft computing based method for vehicles repositioning in bike-sharing systems," *Procedia-Social Behav. Sci.*, vol. 54, pp. 675–684, Oct. 2012.

[5] J. P. Romero, A. Ibeas, J. L. Moura, J. Benavente, and B. Alonso, "A simulation-optimization approach to design efficient systems of bike-sharing," *Procedia-Social Behav. Sci.*, vol. 54, pp. 646–655, Oct. 2012.

[6] K. Liu, Z. X. Xiang, T. Huang, and X. Zhang, "Finite element analysis and improvement of mountain bike frame," *J. Mech. Des.*, vol. 24, no. 3, pp. 39–42, Mar. 2007.

[7] Z. X. Xiang, Y. Bu, Y. H. Zhang, and T. Huang, "Vibrant comfort-based parameterization for mountain bike rear suspension," *J. Tianjin Univ.*, vol. 41, no. 6, pp. 685–689, Jun. 2008.

[8] T. Nakae, T. Ryu, A. Sueoka, Y. Nakano, and T. Inoue, "Squeal and chatter phenomena generated in a mountain bike disc brake," *J. Sound Vibrat.*, vol. 330, no. 10, pp. 2138–2149, May 2011.

[9] D. Covill, S. Begg, E. Elton, M. Milne, R. Morris, and T. Katz, "Parametric finite element analysis of bicycle frame geometries," *Procedia Eng.*, vol. 72, pp. 441–446, Jun. 2014.

[10] Q. C. He, X. M. Fan, D. Z. Ma, and C. Chen, "An investigation of bicycle dynamics in interactive bicycle simulator," *J. Syst. Simul.*, vol. 16, no. 10, pp. 2237–2241, Oct. 2004.

[11] D. J. Huang, T. X. Chen, and Z. Li, "Multidisciplinary design optimization for the truss of bicycle based on Isight," *Manuf. Inf.*, vol. 6, pp. 21–23, Jun. 2015.

[12] W.-H. Du, D.-W. Zhang, L. Zhang, Y.-L. Zhang, and W.-G. Zhang, "Study on mode performance and sensitivity of main frame of electric bicycle," *J. North Univ. China (Natural Sci. Ed.)*, vol. 29, no. 3, pp. 214–218, Mar. 2008.

[13] J. Lépine, Y. Champoux, and J. M. Drouet, "Excitation techniques for testing bike vibration transmission in the laboratory," in *Sensors, Instrumentation and Special Topics*, vol. 6. New York, NY, USA: Springer, 2011, pp. 35–43.

[14] A. Caya, Y. Champoux, and J. M. Drouet, "Dynamic behaviour and measurement accuracy of a bicycle brake hood force transducer," *Procedia Eng.*, vol. 34, pp. 526–531, May 2012.

[15] K. Cui and T. T. Zhao, "Unsaturated dynamic constitutive model under cyclic loading," *Cluster Comput.*, vol. 20, no. 4, pp. 2869–2879, 2017.

[16] Y. G. Sun, H. Y. Qiang, J. Q. Xu, and D. S. Dong, "The nonlinear dynamics and anti-sway tracking control for offshore container crane on a mobile harbor," *J. Marine Sci. Technol.-Taiwan*, vol. 25, no. 6, pp. 656–665, Dec. 2017.

[17] A. E. Alshorbagy, M. A. Eltaher, and F. F. Mahmoud, "Free vibration characteristics of a functionally graded beam by finite element method," *Appl. Math. Model.*, vol. 35, no. 1, pp. 412–425, Jan. 2011.

[18] S. Tao, C. Wu, Z. Sheng, and X. Wang, "Space-time repetitive project scheduling considering location and congestion," *J. Comput. Civil Eng.*, vol. 32, no. 3, pp. 04018017-1–04018017-19, May 2018.

[19] T.-P. Fries and T. Belytschko, "The extended/generalized finite element method: An overview of the method and its applications," *Int. J. Numer. Methods Eng.*, vol. 84, no. 3, pp. 253–304, Aug. 2010.

[20] I. V. Singh, B. K. Mishra, S. Bhattacharya, and R. U. Patil, "The numerical simulation of fatigue crack growth using extended finite element method," *Int. J. Fatigue*, vol. 36, no. 1, pp. 109–119, Mar. 2012.

[21] W.-X. Ren and H.-B. Chen, "Finite element model updating in structural dynamics by using the response surface method," *Eng. Struct.*, vol. 32, no. 8, pp. 2455–2465, Aug. 2010.

[22] C. Gentile, A. Saisi, and A. Cabboi, "Structural identification of a masonry tower based on operational modal analysis," *Int. J. Archit. Heritage*, vol. 9, no. 2, pp. 98–110, May 2012.

[23] K. Cui, W.-H. Yang, and H.-Y. Gou, "Experimental research and finite element analysis on the dynamic characteristics of concrete steel bridges with multi-cracks," *J. Vibroeng.*, vol. 19, no. 6, pp. 4198–4209, Sep. 2017.

[24] J.-Q. Li *et al.*, "An intelligent wireless sensor networks system with multiple servers communication," *Int. J. Distrib. Sensor Netw.*, vol. 11, no. 8, pp. 1–8, Jan. 2015.

[25] K. Yang, N. Yang, C. Xing, J. Wu, and Z. Zhang, "Space-time network coding with transmit antenna selection and maximal-ratio combining," *IEEE Trans. Wireless Commun.*, vol. 14, no. 4, pp. 2106–2117, Dec. 2014.

[26] J. S. Wu, Y. D. Zhang, M. G. Amin, and M. Uysal, "Multiple-relay selection in amplify-and-forward cooperative wireless networks with multiple source nodes," *EURASIP J. Wireless Commun. Netw.*, vol. 2012, pp. 1–13, Aug. 2012.
[27] Q. L. Luo *et al.*, "Reliable broadband wireless communication for high speed trains using baseband cloud," *EURASIP J. Wireless Commun. Netw.*, vol. 2012, pp. 1–12, Sep. 2012.
[28] W. Wei, Z. Sun, H. Song, H. Wang, and X. Fan, "Energy balance-based steerable arguments coverage method in WSNs," *IEEE Access*, to be published, doi: 10.1109/ACCESS.2017.2682845.
[29] J. S. Wu, H. G. Hu, and M. Uysal, "High-rate distributed space-time-frequency coding for wireless cooperative networks," *IEEE Trans. Wireless Commun.*, vol. 10, no. 2, pp. 614–625, Dec. 2010.
[30] W. Wei, J. Su, H. Song, H. Wang, and X. Fan, "CDMA-based anti-collision algorithm for EPC global C1 Gen2 systems," *Telecommun. Syst.*, vol. 67, no. 1, pp. 63–71, Jan. 2018.
[31] R. V. Kulkarni and G. K. Venayagamoorthy, "Particle swarm optimization in wireless-sensor networks: A brief survey," *IEEE Trans. Syst., Man, Cybern. C, Appl. Rev.*, vol. 41, no. 2, pp. 262–267, Jul. 2010.
[32] G. M. Ding, Z. Tan, J. Wu, J. Zeng, and L. Zhang, "Indoor fingerprinting localization and tracking system using particle swarm optimization and Kalman filter," *IEICE Trans. Commun.*, vol. E98B, no. 3, pp. 502–514, Mar. 2015.
[33] J. B. Park, Y.-W. Jeong, J.-R. Shin, and K. Y. Lee, "An improved particle swarm optimization for nonconvex economic dispatch problems," *IEEE Trans. Power Syst.*, vol. 25, no. 1, pp. 156–166, Oct. 2009.
[34] A. Nickabadi, M. M. Ebadzadeh, and R. Safabakhsh, "A novel particle swarm optimization algorithm with adaptive inertia weight," *Appl. Soft Comput.*, vol. 11, no. 4, pp. 3658–3670, Jun. 2011.
[35] J. E. Onwunalu and L. J. Durlofsky, "Application of a particle swarm optimization algorithm for determining optimum well location and type," *Comput. Geosci.*, vol. 14, no. 1, pp. 183–198, Jan. 2010.
[36] B. Xue, M. Zhang, and W. N. Browne, "Particle swarm optimization for feature selection in classification: A multi-objective approach," *IEEE Trans. Cybern.*, vol. 43, no. 6, pp. 1656–1671, Dec. 2012.
[37] G. Zhu and S. Kwong, "Gbest-guided artificial bee colony algorithm for numerical function optimization," *Appl. Math. Comput.*, vol. 217, no. 7, pp. 3166–3173, Dec. 2010.
[38] B. Akay and D. Karaboga, "A modified artificial bee colony algorithm for real-parameter optimization," *Inf. Sci.*, vol. 192, pp. 120–142, Jun. 2012.
[39] B. Akay and D. Karaboga, "Artificial bee colony algorithm for large-scale problems and engineering design optimization," *J. Intell. Manuf.*, vol. 23, no. 4, pp. 1001–1014, Aug. 2012.
[40] K. Cui and X. Qin, "Virtual reality research of the dynamic characteristics of soft soil under metro vibration loads based on BP neural networks," *Neural Comput. Appl.*, vol. 29, no. 5, pp. 1233–1242, Mar. 2018.
[41] W. Y. Szeto, Y. Wu, and S. C. Ho, "An artificial bee colony algorithm for the capacitated vehicle routing problem," *Eur. J. Operat. Res.*, vol. 215, no. 1, pp. 126–135, Nov. 2011.
[42] G. Li, P. Niu, and X. Xiao, "Development and investigation of efficient artificial bee colony algorithm for numerical function optimization," *Appl. Soft Comput.*, vol. 12, no. 1, pp. 320–332, Jan. 2012.
[43] Y. G. Sun, H. Qiang, X. Mei, and Y. Teng, "Modified repetitive learning control with unidirectional control input for uncertain nonlinear systems," *Neural Comput. Appl.*, to be published, doi: 10.1007/s00521-017-2983-y.
[44] M.-A. Hassan, Q.-T. Vien, and M. Aiash, "Software defined networking for wireless sensor networks: A survey," *Adv. Wireless Commun. Netw.*, vol. 3, no. 2, pp. 10–22, Jun. 2017.

ZIDONG HAN received the B.S. degree in electrical engineering from Shanghai Jiao Tong University in 2012 and the M.S. degree in electrical engineering from the National University of Singapore in 2013. He is currently a Senior Research Scholar and an Engineer with the Southern University of Science and Technology, China. He holds over 20 China and U.S. patents, and over 10 PCTs. His research interests include optimization problems for automation and communications systems, machine learning for signal analysis, and the applications of wireless power transfer.

YUFENG LI received the B.S. degree in physics from Shanghai University in 2012 and the M.S. degree in mechanical engineering from The University of Hong Kong in 2013. He is currently an Adjunct Senior Engineer with Shenzhen Hopnetworks Ltd., Shenzhen. His research interests include the adaptive suspension systems of automobiles and machine automation.

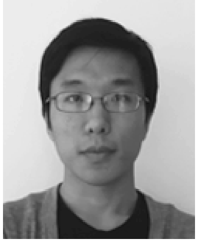

JUNYU LIANG was born in Nanchang , Jiangxi, China. He received the B.Eng. degree in electrical engineering from Nanchang University in 2015. He is currently a Co-Founder and the CEO of Shenzhen Hopnetworks Ltd., Shenzhen. His research interests include the adaptive suspension systems of automobiles and machine automation.